Using short pulses to enhance the production rate of vibrationally excited hydrogen molecules in hydrogen discharge*

Sun Ji-Zhong(孙继忠)†, Li Xian-Tao(李现涛),
Bai Jing(白 净), and Wang De-Zhen(王德真)

School of Physics and Optoelectronic Technology and College of Advanced Science and Technology, Dalian University of Technology, Dalian 116024, *China*

(Received 15 April 2011; revised manuscript received 8 June 2011)

Hydrogen discharges driven by the combined radio-frequency (rf)/short pulse sources are investigated using the particle-in-cell method. The simulation results show that the discharge driven additionally by the short pulse can enhance the electron density and modulate the electron energy to provide a better condition for negative hydrogen ion production than the discharge driven by the rf-only source.

Keywords: hydrogen discharge, particle-in-cell simulation, negative hydrogen ion

PACS: 52.65.Rr, 52.80.–s, 52.25.–b **DOI:** 10.1088/1674-1056/21/5/055205

1. Introduction

Hydrogen discharges have been studied intensively due to their wide applications in material industry, nuclear fusion, and high-energy physics.[1−5] The neutral beam injection is one of the major heating and current driving methods in fusion devices. For fusion reactors like the international thermonuclear experimental reactor (ITER), the beam energy required is up to MeV.[4,5] The neutral beam heating system based on the negative hydrogen ion (NHI) source will replace the one based on the positive hydrogen ion source, since the NHIs can be neutralized efficiently in such an energy range.[6]

Maintenance-free NHI sources are ideal for ITER-like devices. The volume production based NHI sources are preferred,[7] but many issues associated with the hydrogen discharges need to be solved.[8] It is widely received that the major negative hydrogen ion formation mechanism in the pure hydrogen discharge is the dissociative attachment of low energy electrons ($T_e < 1$ eV) to highly vibrationally excited molecules $H_2^*(v)$ (D-A). The $H_2^*(v)$ molecules are mainly populated via the following radiative decay vibrational excitation process (E-V):

$$\begin{aligned} e + H_2(X, \nu = 0) &\rightarrow e + H_2^*(B, C, \cdots) \\ &\rightarrow e + H_2(X, \nu) + h\nu. \end{aligned}$$

This E-V excitation requires a high density of high-energy electrons, while the D-A reaction needs a high density of low-energy electrons.[7] To solve this dilemma, one proposed that the hydrogen discharge could be rapidly pulsed on and off to generate the high-energy and the low-energy electrons respectively.[9] Recently, Sun *et al.*[10] found that in addition to a radio-frequency (rf) power source, a short pulse power source could be employed to modulate the energy of the electrons in the hydrogen discharge. Besides, Bai *et al.*[11] found that the presence of a weak transverse magnetic field could modulate the electron energy and raise the plasma density. In the present paper, we address the hydrogen discharge driven by the combined rf and pulse sources theoretically to demonstrate that with the rf source sustaining the discharge, the short pulse power source can be used to create a favorable condition for H^- production. Considering its important role in generating H^-, we focus our attention on the change in the production rate of $H_2^*(v)$ induced by the pulse source.

2. Simulation model

In the present paper, we use the particle-in-cell/Monte Carlo collision (PIC-MCC) method to investigate the hydrogen discharge driven by the com-

*Project supported by the National Natural Science Foundation of China (Grant No. 10875022).
†Corresponding author. E-mail: jsun@dlut.edu.cn
© 2012 Chinese Physical Society and IOP Publishing Ltd

bined rf and pulse power sources. The PIC method simulates the discharge by recording the particles of interest in the phase space. Typically, the electrons and the ions are tracked, and the neutrals are assumed to form a uniform background. In practice, the so called super particles (each represents a group of charged particles of its kind) are tracked continuously in the phase space by the integration of Newton's equations of motion. The electric potential and the electric field induced by the redistribution of charged particles are evaluated at discrete locations in the position space by solving the Poisson's equation. The Newton's equations of motion and the Poisson's equation constitute a set of self-consistent equations.[12,13] The collision processes undergone by a super particle are handled with the MCC technique.[14] All major chemical reactions associated with the electrons and the vibrationally excited molecules $H_2^*(v)$ are taken into account in the model. The collision reactions are summarized in Table 1.

Table 1. Collision processes considered in the simulation.

Reaction	Process	Reference
Atom elastic collision	$e + H \rightarrow e + H$	[15]
Atom excitation	$e + H \rightarrow e + H^*$	[16]
Atom ionization	$e + H \rightarrow 2e + H^+$	[16]
Vibrational excitation: E-V (via $B_1\Sigma_u^+$, $C^1\Pi_u$)	$e + H_2(v{=}0) \rightarrow e + H_2(w = 0\text{–}14) + hv$	[17]
Electronic excitation: eE (via $B_1\Sigma_u^+$, $C^1\Pi_u$, $B'^1\Sigma_u^+$, $D^1\Pi_u$, $B''^1\Sigma_u^+$, $D'^1\Pi_u$)	$e + H_2(v{=}0) \rightarrow e + H_2$	[17]
Dissociation: eD (via $B_1\Sigma_u^+$, $C^1\Pi_u$, $B'^1\Sigma_u^+$, $D^1\Pi_u$, $B''^1\Sigma_u^+$, $D'^1\Pi_u$, $a^3\Sigma_u^+$, $b^3\Sigma_u^+$, $c^3\Pi_u$)	$e + H_2(v{=}0) \rightarrow e + 2H$	[17], [18]
Molecular ionization: eI	$e + H_2(v{=}0) \rightarrow 2e + H_2^+$	[18]
Dissociative ionization: eDI (via $X^2\Sigma_g^+$,$^2\Sigma_u$)	$e + H_2(v{=}0) \rightarrow 2e + H + H^+$	[18]
Proton excitation: pV	$H^+ + H_2(v{=}0) \rightarrow H^+ + H_2(w = 0\text{–}14)$	[19]
Proton exchange: p-CX	$H^+ + H_2(v{=}0) \rightarrow H + H_2^+$	[20]
Proton impact dissociation: pV-diss	$H^+ + H_2(v{=}0) \rightarrow H + H + H^+$	[21]

The schematic diagram of the simulated system is illustrated in Fig. 1. The hydrogen discharge is generated between two parallel metal plates, the powered one is located at $x = 0$ cm, and the grounded one is located at $x = 20$ cm. The combined rf and pulse power sources are applied to the electrode at $x = 0$ cm. The pulse voltage $V(t)$ is chosen to have a smoothed trapezoidal wave form[22] to eliminate the discontinuity of $\mathrm{d}V(t)/\mathrm{d}t$. The pulse is characterized by rise time t_r, plateau time t_p, and fall time t_f. In this work, we set $t_\mathrm{r} = t_\mathrm{f}$ for simplicity.

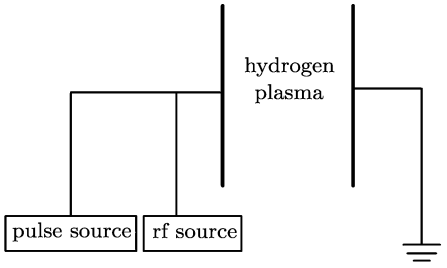


Fig. 1. Schematic diagram of the modeled system. The left electrode is powered by combined pulse and rf power sources, and the right one is electrically grounded.

3. Results and discussion

The simulation parameters are taken as follows. The gas pressure is about 1.6 Pa, the gas temperature is 300 K, and all charged particles are assumed to be absorbed by the electrodes without the secondary electron emission.[23] Initially, the charged particles are distributed uniformly, and their velocities obey the Maxwell distribution. A 13.56 MHz sinusoidal rf source with a voltage amplitude of 500 V and a 135.6 kHz pulse source with a voltage amplitude of –2500 V are used. The pulse duty cycle is set to be 1%, and the pulse rise time and fall time each are 3 ns. The pulse source is assumed to have the same starting phase angle as that of the rf source. Thus, the resulting voltage waveform looks like that shown

in Fig. 2. The simulation is kept running until the discharge reaches a fully periodical state; the data are then extracted from the simulation. To compare with the dual-source powered discharge (referred to as case II), we also simulate the rf source powered only discharge (referred to as case I).

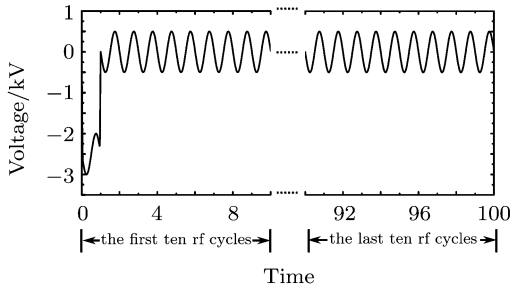


Fig. 2. Jointly applied voltage waveform for one pulse period. Only the first and last ten rf cycles are shown in the figure.

First, we look at the electron density. Both cases show that the quasi-neutral plasma exists in the central part of the discharge gap (which are not shown here), but the plasma densities exhibit a big difference in magnitude, which can be seen clearly from Fig. 3. The electron densities for case II shown in Fig. 3 have been averaged over the first and the last 10 rf cycles (see Fig. 2), respectively. As can be seen, in the first 10 rf cycles, the electron density is approximately 40% higher in case II than that in case I. Even in the last 10 rf cycles, the electron density in case II is still higher than that in case I. This result demonstrates that the electron density can be enhanced by applying an additional pulse power source to the discharge driven by the rf power source.

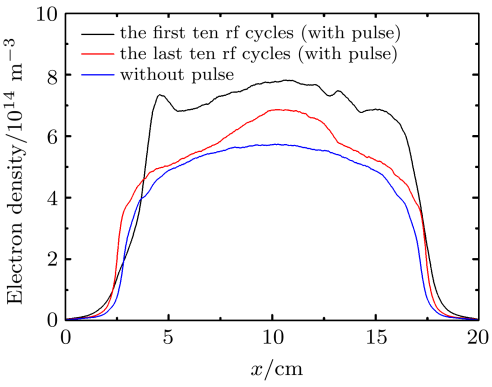


Fig. 3. (colour online) Electron density distributions along the discharge gap.

Now we assess the electron energies in both cases. The mean electron energy is calculated by $\bar{\varepsilon}(t,x) = \int_0^\infty \varepsilon f(t,x,\varepsilon)\mathrm{d}\varepsilon$, where $f(t,x,\varepsilon)$ is the normalized electron energy distribution function (EEDF) at time t and position x. Figure 4 presents the mean electron energies averaged over the first and the last 10 rf cycles in case II , and the mean electron energy averaged over one rf cycle in case I. As shown in Fig. 4, the mean electron energy is remarkably higher in the regions close to the electrodes in both cases, especially, the mean electron energy for the first 10 rf cycles in case II. This phenomenon implies the heating by the time-varying electric field near the sheath region. Interestingly, the mean electron energy in the central part of the discharge gap in the first 10 rf cycles in case II is nearly twice as high as that in case I, but the mean electron energy in the last rf cycle in case II is a little lower than that in case I, which is more evident in the sheath region. This conclusion favors the production of the negative ions via the D-A reaction.

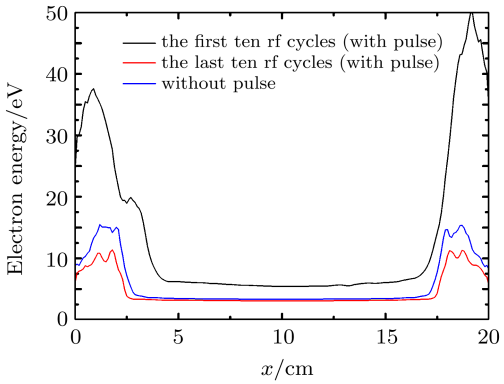


Fig. 4. (colour online) Electron energy distributions along the discharge gap.

Now we study the electric field distribution and try to understand why the electron energy behaves as mentioned above. From Fig. 5, we can see that in the bulk plasma, the electric field is very weak, while in the sheath regions, the electric field is very strong. In reality, the electric field varies with time, and the electrons gain energy from the time-varying electric field, i.e., the so-called stochastic heating. Since in the early rf cycles, the electric field is stronger in case II, then the heating is more powerful. One may observe that for all the energy curves, each has a peak value in the region close to each electrode (see Fig. 4). The exact positions of these peaks are determined by the balance of the energy gained from the electric field and the energy consumed by the collisions. However, the heating of electrons is complicated and will not be discussed

further here.

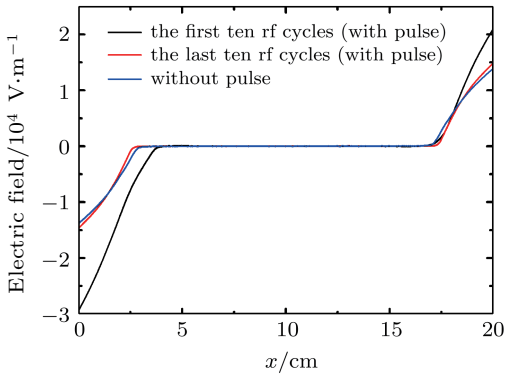


Fig. 5. (colour online) Electric field distributions along the discharge gap.

The vibrationally excited molecules $H_2^*(v)$ play a critical role in producing the negative hydrogen ions and need to be investigated in detail. The $H_2^*(v)$ production rate is contributed to mainly by the E-V reaction, $d[H_2^*(v)]/dt \approx k \cdot n_e \cdot [H_2(0)]$. Since $[H_2(0)]$ is approximately a constant, either quantity k or n_e (or both) can be used to enhance the $H_2^*(v)$ production rate. The reaction rate coefficient k can be evaluated by using integral $k = \int_0^\infty \sigma_{EV}(\varepsilon)\varepsilon^{3/2} f(\varepsilon) d\varepsilon$, where $\sigma_{EV}(\varepsilon)$ is the cross-section of the E-V reaction, and $f(\varepsilon)$ is the EEDF.

Figure 6 displays the $H_2^*(v)$ production rate via the E-V reaction and the mean electron energy averaged over the discharge gap each as a function of time during the first ten rf cycles. In the rf-only discharge, both the electron energy and the $H_2^*(v)$ production rate are virtually independent of time, and are 3.5 eV and 4.0×10^{22} $m^{-3} \cdot s^{-1}$, respectively. In contrast, in the discharge driven by the combined power sources, the values of the two quantities are much higher and depend strongly on time.

Figure 7 shows the $H_2^*(v)$ production rates in the dual-source discharge, which are averaged over the first and the last 10 rf cycles respectively. In Fig. 7, the $H_2^*(\nu)$ production rate in the rf-only discharge is averaged over one rf cycle. As can be seen, the $H_2^*(v)$ production rate in the first 10 rf cycles is 7 times higher in case II than that in case I. If we consider the production rate averaged over the first four rf cycles, the enhancement in the $H_2^*(v)$ production rate by the low duty ratio pulse is even more remarkable. Together with Figs. 3 and 4, we can see that the pulse can enhance the $H_2^*(v)$ production rate greatly via raising the electron energy and density, but this enhancement is obvious only in the early rf cycles, as shown in Fig. 7. Actually, the $H_2^*(v)$ production rate in the later rf cycles is lower, as also can be seen in Fig. 7. With the higher densities of low-energy electrons and $H_2^*(v)$, more negative hydrogen ions can be generated in the later period of every pulse.

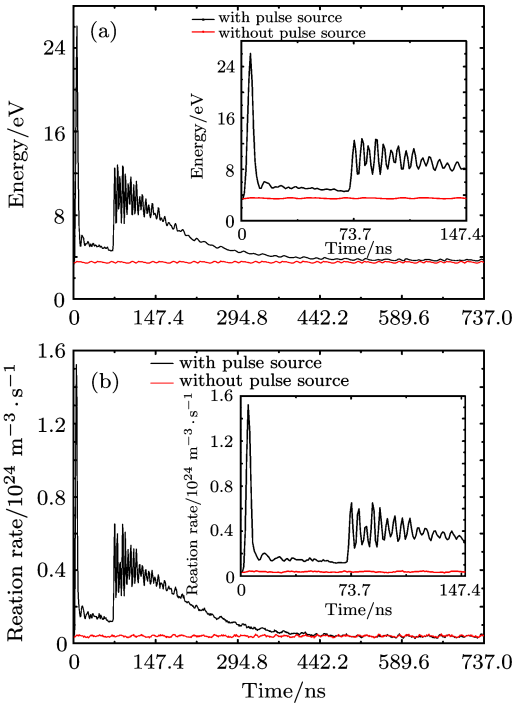


Fig. 6. Time evolutions of (a) the average electron energy and (b) the E-V reaction rate. One rf cycle is about 73.7 ns. The insets show respectively the curves during the first two rf cycles with a magnified time axis.

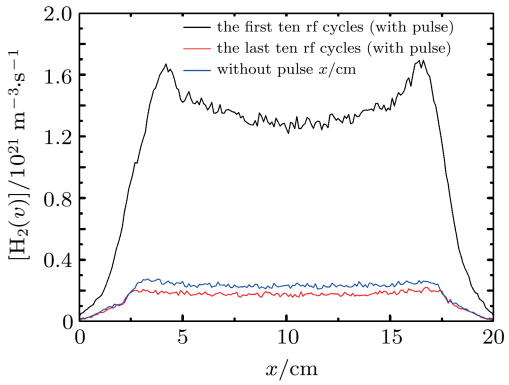


Fig. 7. Production rate of vibrationally excited molecules $H_2^*(v)$ along the discharge gap.

4. Conclusion

In summary, applying a short high voltage pulse to the discharge powered by the rf source can enhance

the production rate of the vibrationally excited hydrogen molecules greatly. The results show that the low duty ratio pulse can raise both the electron density and the electron energy. The enhancement in electron energy leads to a larger reaction rate coefficient of the radiative decay vibrational excitation reaction. At the same time, the low duty ratio pulse leads to a higher density of low-energy electrons in the later pulse-off period, which favors the production of negative hydrogen ions. Further work on the hydrogen discharge driven by the combined sources in a weak transverse magnetic field is under way.

References

[1] Gottscho R A, Preppernau B L, Pearton S J, Emerson A B and Giapis K P 1990 *J. Appl. Phys.* **68** 440

[2] Bachmann P K, Leers D and Lydtin H 1991 *Diamond Relat. Mater.* **1** 1

[3] Aoki Y, Aoyama S, Uetake H, Morizuka K and Ohmi T 1993 *J. Vac. Sci. Technol.* A **11** 307

[4] Hemsworth R S and Inoue T 2005 *IEEE Trans. Plasma Sci.* **33** 1799

[5] Fantz U, Franzen P, Kraus W, Berger M, Christ-Koch S, Falter H, Fröschle M, Gutser R, Heinemann B, Martens C, McNeely P, Riedl R, Speth E, Stäbler A and Wünderlich D 2009 *Nucl. Fusion* **49** 125007

[6] Kuriyama M, Akino N, Aoyagi T, Ebisawa N, Isozaki N, Honda A, Inoue T, Itoh T, Kawai M, Kazawa M, Koizumi J, Mogaki K, Ohara Y, Ohga T, Okumura Y, Oohara H, Ohshima K, Satoh F, Takenouchi T, Toyokawa Y, Usui K, Watanabe K, Yamamoto M, Yamazaki T and Zhou C 1998 *Fusion Eng. Des.* **39–4** 115

[7] Bacal M 2006 *Nucl. Fusion* **46** S250

[8] Capitelli M and Gorse C 2005 *IEEE Trans. Plasma Sci.* **33** 1832

[9] Hopkins M B and Mellon K N 1991 *Phys. Rev. Lett.* **67** 449

[10] Sun I Z, Li X T, Sang C F, Jiang W, Zhang P Y and Wang D Z 2010 *Phys. Plasmas* **17** 103505

[11] Bai J, Sun J Z, Zhang Q Z and Wang D Z 2011 *Curr. Appl. Phys.* **11** S140

[12] Birdsall C K and Langdon A B 1985 *Plasma Physics via Computer Simulation* (New York: McGraw-Hill)

[13] Verboncoeur J P 2005 *Plasma Phys. Control. Fusion* **47** A231

[14] Vahedi V and Surendra M 1995 *Comput. Phys. Commun.* **87** 179

[15] Janev R K, Reiter D and Samm U 2003 *Collision Process in Low-temperature Hydrogen Plasmas Berichte des Forschungszentrums Jülich* Jül-4105

[16] http://srdata.nist.gov/gateway/gateway?keyword=ionization

[17] Celiberto R, Janev R, Laricchiuta A, Capitelli M, Wadehra J and Atems D 2001 *Atom. Data Nucl. Data* **77** 161

[18] Celiberto R, Capitelli M and Laricchiuta A 2002 *Phys. Scr.* **96** 31

[19] http://www-cfadc.phy.ornl.gov/cgi-bin/kmolh2-scl.cgi

[20] Krstić P S, Schultz D R and Janev R K 2002 *Phys. Scr.* **96** 61

[21] Krstić P S and Janev R K 2003 *Phys. Rev.* A **67** 22708

[22] Stewart R A and Lieberman M A 1991 *J. Appl. Phys.* **70** 3481

[23] Lieberman M A and Lichtenberg A J 2005 *Principles of Plasma Discharges and Materials Processing* (2nd Edn.) (New York: Wiley-Interscience) pp. 396–429